The calcium sensor STIM1 is an essential mediator of arterial thrombosis and ischemic brain infarction

David Varga-Szabo,[1] Attila Braun,[1] Christoph Kleinschnitz,[2] Markus Bender,[1] Irina Pleines,[1] Mirko Pham,[3,5] Thomas Renné,[4] Guido Stoll,[2] and Bernhard Nieswandt[1,4]

[1]Rudolf Virchow Center, DFG Research Center for Experimental Biomedicine, [2]Department of Neurology, [3]Department of Neuroradiology, and [4]Institute of Clinical Biochemistry and Pathobiochemistry, University of Würzburg, 97078 Würzburg, Germany
[5]Department of Neuroradiology, University of Heidelberg, 69120 Heidelberg, Germany

Platelet activation and aggregation are essential to limit posttraumatic blood loss at sites of vascular injury but also contributes to arterial thrombosis, leading to myocardial infarction and stroke. Agonist-induced elevation of $[Ca^{2+}]_i$ is a central step in platelet activation, but the underlying mechanisms are not fully understood. A major pathway for Ca^{2+} entry in nonexcitable cells involves receptor-mediated release of intracellular Ca^{2+} stores, followed by activation of store-operated calcium (SOC) channels in the plasma membrane. Stromal interaction molecule 1 (STIM1) has been identified as the Ca^{2+} sensor in the endoplasmic reticulum (ER) that activates Ca^{2+} release–activated channels in T cells, but its role in mammalian physiology is unknown. Platelets express high levels of STIM1, but its exact function has been elusive, because these cells lack a normal ER and Ca^{2+} is stored in a tubular system referred to as the sarcoplasmatic reticulum. We report that mice lacking STIM1 display early postnatal lethality and growth retardation. STIM1-deficient platelets have a marked defect in agonist-induced Ca^{2+} responses, and impaired activation and thrombus formation under flow in vitro. Importantly, mice with STIM1-deficient platelets are significantly protected from arterial thrombosis and ischemic brain infarction but have only a mild bleeding time prolongation. These results establish STIM1 as an important mediator in the pathogenesis of ischemic cardio- and cerebrovascular events.

CORRESPONDENCE
Bernhard Nieswandt:
bernhard.nieswandt@
virchow.uni-wuerzburg.de

Platelet activation and aggregation at sites of vessel wall injury is crucial to prevent posttraumatic blood loss, but it also causes precipitate diseases such as myocardial infarction and stroke, which are still leading causes of death and disability in industrialized countries (1). Inhibition of platelet function is an important strategy for the prevention and treatment of myocardial infarction (2) and, possibly, stroke (2, 3). Platelet activation is triggered by subendothelial collagens, thromboxane A_2 (TxA_2) and ADP released from activated platelets, and thrombin generated by the coagulation cascade (4). Although these agonists trigger different signaling pathways, all activate phospholipase Cs (PLCs), leading to the production of diacylglycerol (DAG) and inositol 1,4,5-triphosphate (IP_3). IP_3 induces the release of Ca^{2+} from the sarcoplasmatic reticulum (SR), which is thought to trigger the influx of extracellular Ca^{2+} by a mechanism known as store-operated Ca^{2+} entry (SOCE) (5, 6). In addition, DAG and some of its metabolites have been shown to induce non-SOCE (7). Stromal interaction molecule 1 (STIM1) is an SR/endoplasmic reticulum (ER)–resident protein necessary for the detection of ER Ca^{2+} depletion and the activation of SOC channels in T cells (8–10) and mast cells (11). In human T cells, the four transmembrane–domain protein Orai1 (Ca^{2+} release–activated channel modulator) appears to be the predominant SOC channel (12), but the C-terminal region of STIM1 also interacts with other SOC channel candidates, such as transient receptor potential channels (TRPCs) 1, 2, and 4 (13). In platelets, STIM1 is expressed at high levels (14) and may

D. Varga-Szabo and A. Braun contributed equally to this paper.
The online version of this article contains supplemental material.

The Journal of Experimental Medicine

contribute to SOCE by interacting with TRPC1 (15). We recently reported that mice expressing an activating EF-hand mutant of STIM1 have elevated $[Ca^{2+}]_i$ levels in platelets, macrothrombocytopenia, and a bleeding disorder, indicating a role for STIM1-dependent SOCE in platelet function (14). The importance of SOCE for platelet activation, hemostasis, and thrombosis, however, remains unknown, and the mechanisms underlying the process are not defined.

RESULTS AND DISCUSSION

To address the function of STIM1 in vivo, the *Stim1* gene was disrupted in mice by insertion of an intronic gene trap cassette. Mice heterozygous for the STIM1-null mutation developed normally, whereas a majority (~70%) of mice lacking STIM1 (*Stim1*$^{-/-}$) died within a few hours after birth. Marked cyanosis was noted before death, suggesting a cardiopulmonary defect. Surviving *Stim1*$^{-/-}$ mice exhibited marked growth retardation, achieving ~50% of the weight of wild-type littermates at 3 and 7 wk of age (Fig. 1, A and B). Western blot analyses confirmed the absence of STIM1 in platelets (Fig. 1 C, top) and other tissues (not depicted). Blood platelet counts (Fig. 1 D), mean platelet volume, and expression levels of major platelet surface receptors, including glycoprotein (GP) Ib-V-IX, GPVI, CD9, and β1 and β3 integrins (not depicted)

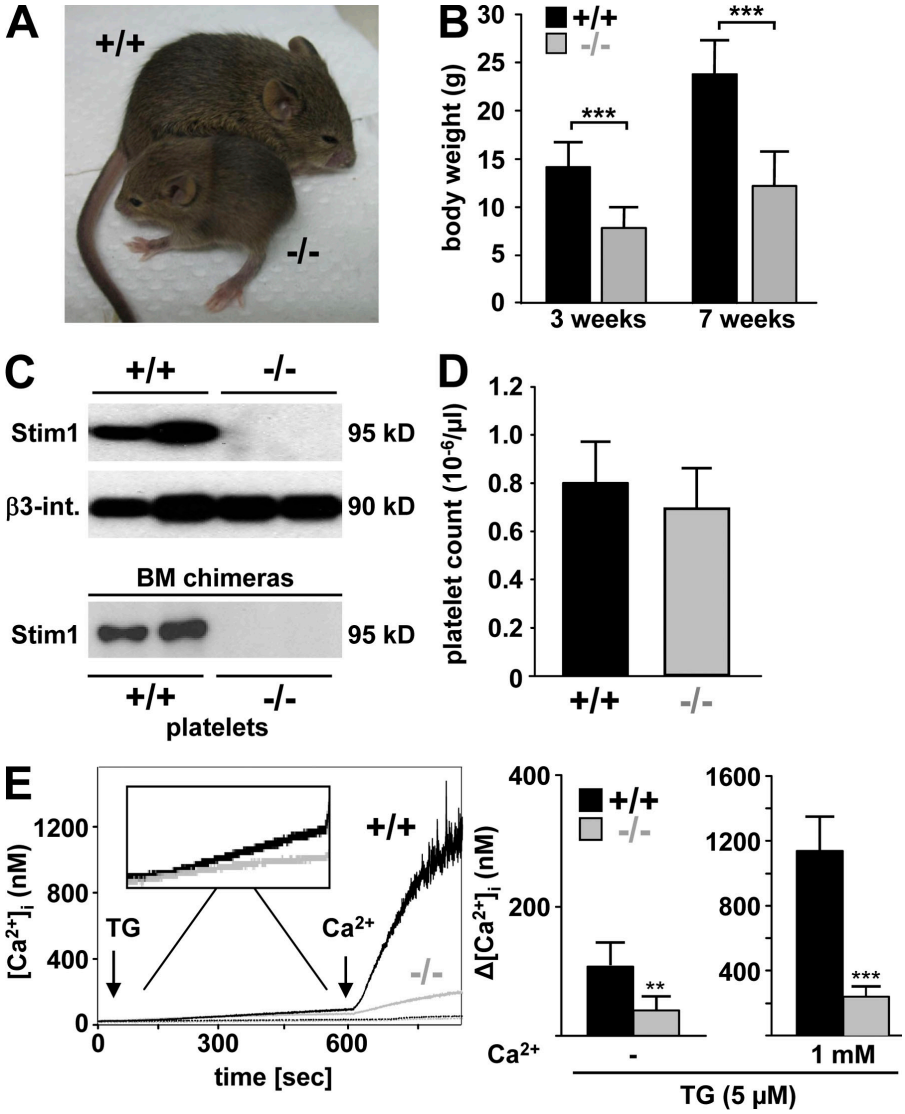

Figure 1. Defective SOCE in Stim1-deficient platelets. (A) 5-wk-old wild-type and *Stim1*$^{-/-}$ littermates. (B) Body weights of wild-type (+/+) and *Stim1*$^{-/-}$ (−/−) mice. Values are mean ± SD. ***, P < 0.001. (C) Western blot analyses of platelet lysates from mice with the indicated genotypes (top) or of mice transplanted with the indicated bone marrow (bottom). Stim1 was assessed using an antibody that can recognize the N-terminal region of the protein (GOK/Stim1; reference 11). An antibody to β3 integrin served as control. Results from two individuals per group are shown. (D) Peripheral platelet counts in wild-type and *Stim1*$^{-/-}$ mice. Values are mean ± SD. (E) Fura-2–loaded platelets were stimulated with 5 µM TG for 10 min, followed by the addition of extracellular Ca^{2+} and monitoring of $[Ca^{2+}]_i$. Representative measurements (left) and maximal increase in intracellular Ca^{2+} concentrations compared with baseline levels ($\Delta[Ca^{2+}]_i$) ± SD (n = 4 mice per group) before and after addition of 1 mM Ca^{2+} (right) are shown. **, P < 0.01; ***, P < 0.001.

were normal, indicating that STIM1 is not essential for megakaryopoiesis or platelet production. Similarly, no differences were found in red blood cell counts, hematocrit, or the activated partial thromboplastin time, a method for the assessment of plasma coagulation (Table I). To determine if STIM1 has a role in platelet SOCE, we induced SOC influx in wild-type and *Stim1*$^{-/-}$ platelets with the SR/ER Ca^{2+} ATPase (SERCA) pump inhibitor thapsigargin (TG). Interestingly, TG-induced Ca^{2+} store release was reduced ~60% in *Stim1*$^{-/-}$ platelets compared with wild-type controls (Fig. 1 E). Furthermore, subsequent TG-dependent SOC influx was almost completely absent in *Stim1*$^{-/-}$ cells (Fig. 1 E). This demonstrates for the first time that STIM1 is essential for SOCE in platelets and suggests that STIM1-dependent processes contribute to the regulation of Ca^{2+} store content in these cells.

Defective SOC influx in *Stim1*$^{-/-}$ platelets

Because of the early mortality and pronounced growth retardation in *Stim1*$^{-/-}$ mice, all subsequent studies were performed with lethally irradiated wild-type mice transplanted with *Stim1*$^{-/-}$ or wild-type bone marrow. 4 wk after transplantation, platelet counts were normal and STIM1 deficiency in platelets was confirmed by Western blotting (Fig. 1 C, bottom). To determine the significance of defective SOCE for agonist-induced platelet activation, we assessed changes in $[Ca^{2+}]_i$ in response to ADP, thrombin, a collagen-related peptide (CRP) that stimulates the collagen receptor GPVI (Fig. 2, A and B), and the TxA_2 analogue U46619 (not depicted). Ca^{2+} release from intracellular stores was reduced in *Stim1*$^{-/-}$ platelets compared with control for all agonists, indicating reduced Ca^{2+} levels in stores in *Stim1*$^{-/-}$ cells. In the presence of extracellular calcium, Ca^{2+} influx was dramatically reduced in *Stim1*$^{-/-}$ platelets. Thus, STIM1-dependent SOCE is a crucial component of the Ca^{2+} signaling mechanism in platelets for all major agonists, and non-SOCE makes only a minor contribution, at least under the conditions tested.

STIM1 in platelet activation and thrombus formation

To test the functional consequences of this defect, we performed ex vivo aggregation studies. *Stim1*$^{-/-}$ platelets aggregated normally to the G protein–coupled agonists ADP, thrombin (Fig. 2 C), and U46619 (not depicted), even at very low concentrations of these agonists (not depicted). In contrast, responses to collagen and CRP (Fig. 2 C) and the strong GPVI agonist convulxin (not depicted) were significantly diminished. The activation defect was confirmed by flow cytometric analysis of integrin αIIbβ3 activation using the JON/A-PE antibody, and of degranulation-dependent P-selectin surface exposure (Fig. 2 D). Therefore, loss of STIM1-dependent SOCE impairs GPVI-induced integrin activation and degranulation, whereas G protein–coupled agonists are still able to induce normal activation in *Stim1*$^{-/-}$ platelets in these assays, despite the defect in $[Ca^{2+}]_i$ signaling.

In vivo, platelet activation on the extracellular matrix or a growing thrombus occurs in flowing blood, where locally produced soluble mediators are rapidly cleared. Under these conditions, reduced potency of platelet activators may become limiting, particularly at the high flow rates found in arteries and arterioles. Therefore, we analyzed the ability of *Stim1*$^{-/-}$ platelets to form thrombi on collagen-coated surfaces in a whole-blood perfusion system (16). Under high shear conditions (1,700 s^{-1}), wild-type platelets adhered to collagen fibers and formed aggregates within 2 min that consistently grew into large thrombi by the end of the perfusion period (Fig. 2 E). In sharp contrast, *Stim1*$^{-/-}$ platelets exhibited reduced adhesion, and three-dimensional growth of thrombi was markedly impaired. As a consequence, the surface area covered by platelets and the total thrombus volume were reduced ~42 and ~81%, respectively. Similar results were obtained at intermediate shear rates (1,000 s^{-1}; not depicted). These findings indicate that STIM1-mediated SOCE is required for efficient platelet activation on collagen and on the surface of growing thrombi under conditions of high shear.

Unstable arterial thrombi in *Stim1*$^{-/-}$ mice

Because platelet aggregation may contribute to pathological occlusive thrombus formation, we studied the effects of STIM1 deficiency on ischemia and infarction by in vivo fluorescence microscopy after ferric chloride–induced mesenteric arteriole injury. In all wild-type chimeras, the formation of small aggregates was observed ~5 min after injury, with progression to complete vessel occlusion in 8 out of 10 mice within 30 min (mean occlusion time = 16.5 ± 2.8 min; Fig. 3, A–C). In contrast, aggregate formation was significantly delayed in ~50% of the *Stim1*$^{-/-}$ chimeras (10.6 ± 5.8 min in wild-type and 17.1 ± 7.3 min in *Stim1*$^{-/-}$ chimeras until the first thrombus >20 μm in diameter appeared; $P < 0.05$), and formation of stable thrombi was almost completely abrogated. This defect was caused by the release of individual platelets from the surface of the thrombi (Videos 1 and 2, available at http://www.jem.org/cgi/content/full/jem.20080302/DC1) and not by embolization of large thrombus fragments. Blood flow was maintained throughout the observation period in 9 out of 10 vessels, demonstrating a crucial role for STIM1 during occlusive thrombus formation. This was confirmed in a second arterial thrombosis model in which the abdominal aorta was mechanically injured and blood flow was monitored with an ultrasonic flow probe.

Table I. Hematology and hemostasis in *Stim1*$^{-/-}$ chimeras

	Stim1$^{+/+}$	*Stim1*$^{-/-}$
Erythrocytes	8,450 ± 139	8,250 ± 264
HCT (%)	40.8 ± 0.4	41.7 ± 1.9
aPTT (sec)	37.7 ± 5.1	38.7 ± 3.1
PT (sec)	9.4 ± 0.5	9.8 ± 0.7
TCT (sec)	19.2 ± 2.6	21.8 ± 1
Fibrinogen	2.2 ± 0.1	2.8 ± 0.6

Erythrocyte counts per nanoliter and coagulation parameters for control and *Stim1*$^{-/-}$ chimeras are shown. Values are mean ± SD of five mice for each genotype. aPTT, activated partial thromboplastin time; HCT, hematocrit; PT, prothrombin time; TCT, thrombin clotting time.

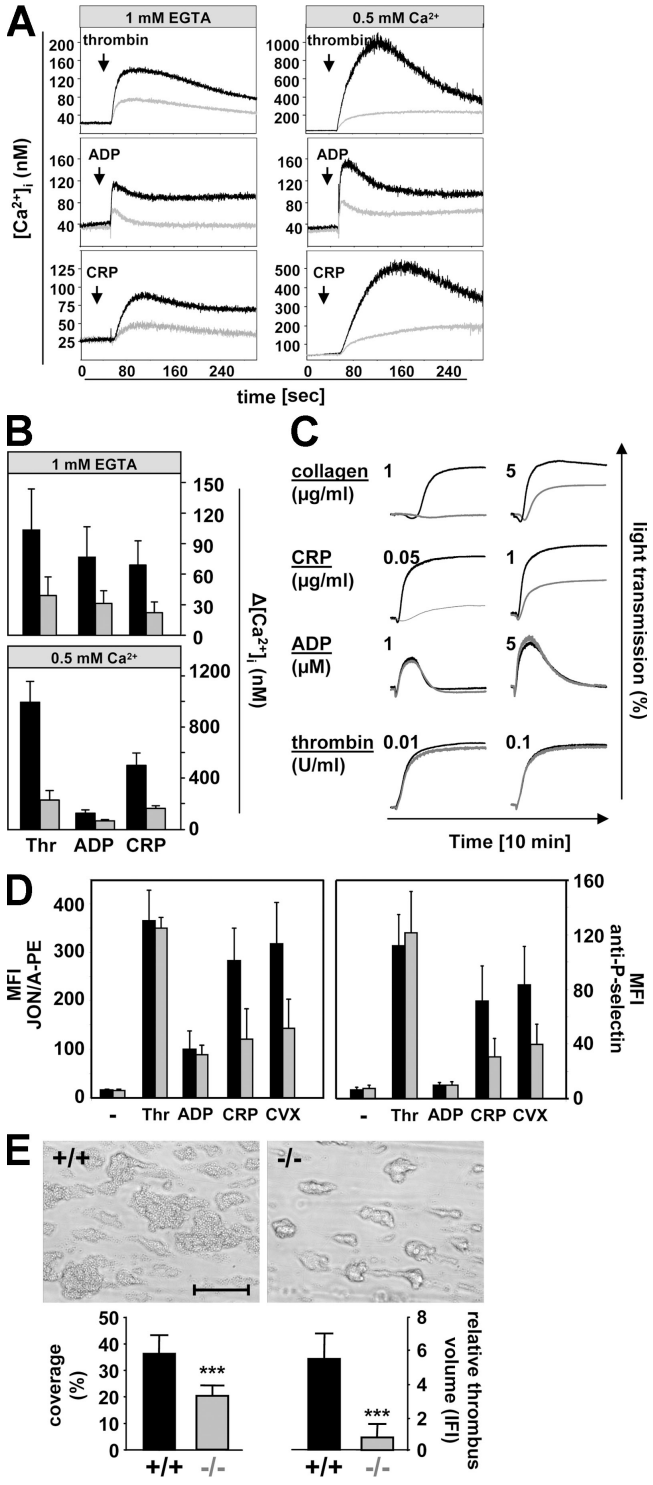

Figure 2. Defective agonist-induced Ca^{2+} signaling and aggregate formation under flow in *Stim1*$^{-/-}$ platelets. Fura-2–loaded wild-type (black line) or *Stim1*$^{-/-}$ (gray line) platelets were stimulated with 0.1 U/ml thrombin, 10 μM ADP, or 10 μg/ml CRP in the presence of extracellular 1 mM EGTA or 0.5 mM Ca^{2+}, and $[Ca^{2+}]_i$ was monitored. Representative measurements (A) and maximal increase in intracellular Ca^{2+} concentrations compared with baseline levels before stimulus ($\Delta[Ca^{2+}]_i$) ± SD (n = 4 mice per group; B) are shown. (C) Impaired aggregation of *Stim1*$^{-/-}$ platelets (gray lines) in response to CRP and collagen but not ADP and thrombin (recording time = 10 min). (D) Flow cytometric analysis of integrin αIIbβ3 activation (binding of JON/A-PE; left) and degranulation-dependent P-selectin exposure (right) in response to 0.1 U/ml thrombin, 10 μM ADP, 10 μg/ml CRP, and 1 μg/ml convulxin. Results are means ± SD (n = 6 mice per group). (E) *Stim1*$^{-/-}$ platelets in whole blood fail to form stable thrombi when perfused over a collagen-coated (0.2 mg/ml) surface at a shear rate of 1,700 s^{-1}. (top) Representative phase-contrast images. (bottom) Mean surface coverage (left) and relative platelet deposition as measured by the integrated fluorescent intensity per square millimeter (right) ± SD (n = 4 mice). ***, $P < 0.001$. Bar, 100 μm.

Although 10 out of 11 control chimeras formed irreversible occlusions within 16 min (mean occlusion time = 4.4 ± 4.1 min), occlusive thrombus formation did not occur in 6 out of 8 *Stim1*$^{-/-}$ chimeras during the 30-min observation period ($P < 0.005$; Fig. 3, D and E). These results demonstrate that STIM1 is required for the propagation and stabilization of platelet-rich thrombi in small and large arteries, irrespective of the type of injury.

To test whether the defect in *Stim1*$^{-/-}$ platelets impaired hemostasis, we measured tail bleeding times. Although bleeding stopped in 28 out of 30 (93.3%) control mice within 10 min, bleeding was highly variable in *Stim1*$^{-/-}$ chimeras, with 11 out of 31 (35.5%) mice bleeding for >10 min ($P < 0.02$; Fig. 3 F). These results show that STIM1 is required for normal hemostasis.

STIM1 is an essential mediator of ischemic brain infarction

Ischemic stroke is the third leading cause of death and disability in industrialized countries (17). Although it is well established that microvascular integrity is disturbed during cerebral ischemia (18), the signaling cascades involved in intravascular thrombus formation in the brain are poorly understood. To determine the importance of STIM1-dependent SOCE in this process, we studied the development of neuronal damage in *Stim1*$^{-/-}$ chimeras after transient cerebral ischemia in a model that depends on thrombus formation in microvessels downstream from a middle cerebral artery (MCA) occlusion (19). To initiate transient cerebral ischemia, a thread was advanced through the carotid artery into the MCA and allowed to remain for 1 h (transient MCA occlusion [tMCAO]), reducing regional cerebral flow by >90% (3). In *Stim1*$^{-/-}$ chimeras, infarct volumes 24 h after reperfusion, as assessed by 2,3,5-triphenyltetrazolium chloride (TTC) staining, were reduced to <30% of the infarct volumes in control chimeras (17 ± 4.4 vs. 62.9 ± 19.3 mm^3; $P < 0.0001$; Fig. 4 A). Reductions in infarct size were functionally relevant, as the Bederson score assessing global neurological function (1.86 ± 0.48 vs. 3.07 ± 0.35, respectively; $P < 0.0001$) and the grip test, which specifically measures motor function and coordination (3.71 ± 0.39 vs. 2 ± 0.65, respectively; $P < 0.0001$), were significantly better in *Stim1*$^{-/-}$ chimeras compared with controls (Fig. 4, B and C). Serial magnetic resonance imaging (MRI) on living mice was used to confirm the protective effect of STIM1 deficiency on infarct development. Hyperintense ischemic infarcts on T2-weighted (T2-w) MRI

in *Stim1*$^{-/-}$ chimeras were <10% of the size of infarcts in control chimeras 24 h after tMCAO ($P < 0.0001$; Fig. 4 D). Importantly, infarct volume did not increase between days 1 and 7, indicating a sustained protective effect for STIM1 deficiency. Moreover, no intracranial hemorrhage was detected on T2-w gradient echo images, a highly sensitive MRI sequence for the detection of blood (Fig. 4 D), indicating that STIM1 deficiency in hematopoietic cells is not associated with an increase in

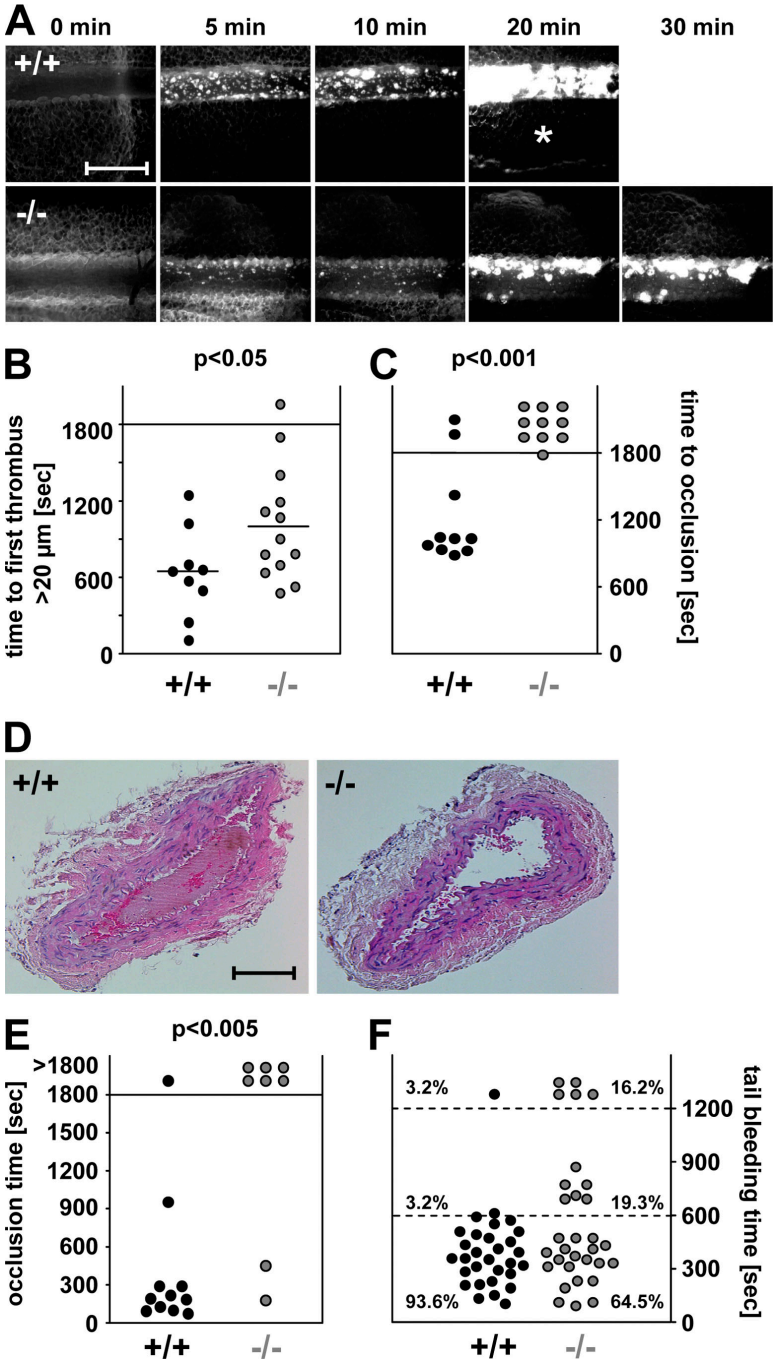

Figure 3. In vivo analysis of thrombosis and hemostasis. (A–C) Mesenteric arterioles were treated with $FeCl_3$, and adhesion and thrombus formation of fluorescently labeled platelets were monitored by in vivo video microscopy. Representative images (A), the time to appearance of the first thrombus >20 µm (B), and the time to vessel occlusion (C) are shown. Each symbol represents one individual. The asterisk in A indicates occlusion of the vessel. Horizontal bars in B represent means. Bar, 50 µm. (D and E) The abdominal aorta was mechanically injured, and blood flow was monitored for 30 min or until complete occlusion occurred (blood flow stopped >5 min). (D) Representative cross sections of the abdominal aorta of mice with wild-type or *Stim1*$^{-/-}$ platelets 30 min after injury. Bar, 250 µm. (E) Time to vessel occlusion. Each symbol represents one individual. (F) Tail bleeding times in wild-type and *Stim1*$^{-/-}$ chimeras. Each symbol represents one individual. Videos 1 and 2 are available at http://www.jem.org/cgi/content/full/jem.20080302/DC1.

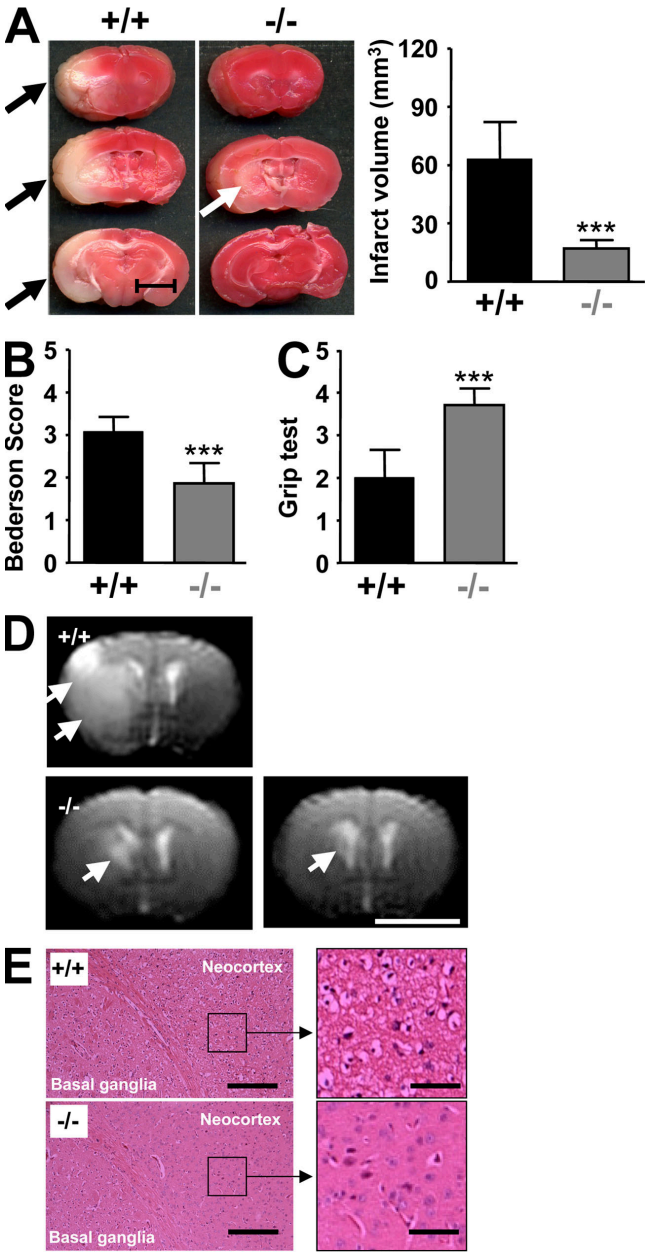

Figure 4. *Stim1*$^{-/-}$ chimeras are protected from cerebral ischemia. (A, left) Representative images of three corresponding coronal sections from control mice and *Stim1*$^{-/-}$ chimeras stained with TTC 24 h after tMCAO. Infarcts in *Stim1*$^{-/-}$ chimeras are restricted to the basal ganglia (white arrow), in contrast to controls (black arrows). (right) Brain infarct volumes in controls ($n = 7$) and *Stim1*$^{-/-}$ chimeras ($n = 7$). Values are mean ± SD. ***, $P < 0.0001$. Bar, 5 mm. (B and C) Neurological Bederson score and grip test assessed at day 1 after tMACO of controls ($n = 7$) and *Stim1*$^{-/-}$ chimeras ($n = 7$). Values are mean ± SD. ***, $P < 0.0001$. (D) The coronal T2-w MR brain image shows a large hyperintense ischemic lesion at day 1 after tMCAO in controls (white arrows; top left). Infarcts are smaller in *Stim1*$^{-/-}$ chimeras (white arrow; bottom left), and T2 hyperintensity decreases by day 7 during infarct maturation (white arrow; bottom right). Importantly, hypointense areas indicating intracerebral hemorrhage were not seen in *Stim1*$^{-/-}$ chimeras, demonstrating that Stim1 deficiency does not increase the risk of hemorrhagic transformation, even at advanced stages of infarct development. Bar, 5 mm. (E) Hematoxylin and eosin–stained sections of corresponding territories in the ischemic hemispheres of control and *Stim1*$^{-/-}$ chimeras. Infarcts are restricted to the basal ganglia in *Stim1*$^{-/-}$ chimeras but consistently include the cortex in controls. Bars: (left) 200 µm; (right) 50 µm.

bleeding complications in the brain. Consistent with the TTC stains and MRI images, histological analysis revealed massive ischemic infarction of the basal ganglia and neocortex in control chimeras but only limited infarction of the basal ganglia in *Stim1*$^{-/-}$ chimeras (Fig. 4 E). The density of CD3$^+$ T cell and monocyte/macrophage infiltrates in brain infarcts was low, and did not differ between *Stim1*$^{-/-}$ and control chimeras at 24 h (not depicted).

STIM1 has been identified as the long-sought calcium sensor that connects intracellular Ca^{2+} store depletion to the activation of plasma membrane SOC channels in immune cells. Although SOCE is thought to be a major pathway of Ca^{2+} entry in virtually all nonexcitable cells, this has only been directly shown for T cells (8–10) and IgE-dependent mast cell activation (11). Although STIM1 is highly expressed in platelets (14), the significance of SOCE for platelet function has been unknown because non-SOCE pathways have been described to exist in these cells (20). We found severely defective Ca^{2+} responses to all major agonists in *Stim1*$^{-/-}$ platelets, clearly establishing SOCE as the major route of Ca^{2+} entry in those cells and STIM1 as an essential mediator of this process. The residual Ca^{2+} influx detected in the mutant cells suggests that other molecules may regulate SOC influx, but only to a minor extent. One candidate molecule is STIM2, which has been shown to activate Ca^{2+} release–activated channels (21). Alternatively, the residual Ca^{2+} entry could be mediated by store-independent mechanisms as DAG, and some of its metabolites have been shown to induce non-SOCE (7). In line with this, members of the TRPC family have been suggested as candidates mediating both SOCE and non-SOCE in platelets (15, 20).

Besides the severely impaired SOCE, we also observed reduced Ca^{2+} release from intracellular stores upon agonist-induced platelet activation, which likely reflects a lower filling state of the SR, as shown by passively emptying the stores with the SERCA inhibitor TG (Fig. 1 E). Similar observations have very recently been reported in mast cells (11), indicating that STIM1 may be involved in the filling of intracellular Ca^{2+} stores. However, mast cells lacking the major SOC channel Orai1 (22) show normal store content, suggesting a SOC channel–independent role of STIM1 in store refill, possibly through interaction with the IP_3 receptors or SERCA pumps in the SR/ER. Because platelets do not have a normal ER, an interesting question is where STIM1 is located in these cells. The major intracellular Ca^{2+} store seems to be in the so-called dense tubular system, an equivalent of the ER in megakaryocytes. However, lysosome-related (acidic) organelles have been proposed as a second source of intracellularly stored Ca^{2+} in platelets. Further studies are required to clarify the exact location of STIM1 in platelets.

Although STIM1 deficiency severely reduced Ca^{2+} entry in platelets in response to all agonists tested, it did not impair G protein–coupled receptor (GPCR)/PLCβ−triggered integrin αIIbβ3 activation or release of granule content in the absence of flow (Fig. 2), even at very low agonist concentrations (not depicted). This shows that SOCE is not essential for these processes when the agonist can act on the cells at constant concentrations for a prolonged period of time. In contrast, GPVI/PLCγ2-induced cellular activation was impaired under these experimental conditions, even at very high agonist concentrations (Fig. 2 C). The reason for this is not clear at present, but it could be related to the fact that GPVI and GPCRs activate different PLC isoforms in platelets. GPVI ligation triggers tyrosine phosphorylation cascades downstream of the receptor-associated immunoreceptor tyrosine-based activation motif (ITAM), culminating in the activation of PLCγ2 (23), whereas soluble agonists such as thrombin, ADP, and TxA_2 stimulate receptors that couple to heterotrimeric G proteins (Gq) and lead to activation of PLCβ (24). Our Ca^{2+} measurements show that store release and subsequent SOC influx occur significantly faster upon Gq/PLCβ stimulation compared with GPVI/PLCγ2 stimulation (Fig. 2 A), suggesting different kinetics of IP_3 production between these two pathways that could influence subsequent events. Clearly, the low $[Ca^{2+}]_i$ levels alone cannot explain the defective activation downstream of GPVI/PLCγ2, as similar or lower levels are seen in response to thrombin and ADP, respectively, without causing this defect. Possibly, elevated $[Ca^{2+}]_i$ levels have to act in concert with other transient signals, which may not or no longer be fully present in GPVI/PLCγ2-stimulated *Stim1*$^{-/-}$ platelets. This could also explain why platelets expressing an activating EF-hand mutant of STIM1 that leads to elevated basal $[Ca^{2+}]_i$ levels display a selective GPVI/PLCγ2 signaling defect, whereas Gq/PLCβ-induced store release and Ca^{2+} entry are largely preserved (14).

The rather moderate activation deficits seen in *Stim1*$^{-/-}$ platelets in the absence of flow translated into severely defective formation of stable three-dimensional thrombi under conditions of medium and high shear (Fig. 3). Such a phenotype has previously been reported in several mice with deficiencies in platelet proteins, including those lacking the heterotrimeric G protein subunit G_{13} or CD40 ligand, which display marked defects in thrombus stability under flow in vitro and in vivo despite only mild defects in activation/aggregation in the absence of flow (for review see reference 4). This suggests that STIM1-dependent SOCE is particularly important under conditions where agonist potency becomes limiting because of rapid dilution and various stimuli have to be integrated to produce an appropriate cellular response (24). Reduced exposure times rather than low concentrations of these soluble agonists appear to cause the defect under flow, as we observed no reduction in the aggregation response to GPCR activation in *Stim1*$^{-/-}$ platelets, even at very low agonist concentrations (not depicted). In addition, STIM1 may be involved in the generation of Ca^{2+} signals downstream of GPIb, which is essential for adhesion and thrombus formation under flow but is not required for the activation and aggregation of platelets in the absence of shear forces (1, 25).

Our data indicate that STIM1-dependent SOCE may be of greater relevance for arterial occlusive thrombus formation than for primary hemostasis, though prolonged tail bleeding was observed in a subgroup of *Stim1*$^{-/-}$ chimeras (Fig. 3). This raises the interesting possibility that hemostasis and thrombosis are mechanistically distinct processes. Therefore, the identification of the mechanisms that trigger pathological thrombus formation but are less essential to arrest bleeding may be the key to the development of safe antithrombotics. This will be of particular importance for the treatment of acute stroke, which is still the third leading cause of death and disability in industrialized countries, with very limited treatment options (17). Numerous attempts to attenuate infarct progression in acute stroke patients by conventional platelet aggregation inhibitors or anticoagulation failed because of an excess of intracerebral hemorrhages (26). We found that *Stim1*$^{-/-}$ chimeras are protected from neuronal damage after transient cerebral ischemia without displaying an increased risk of intracranial hemorrhage (Fig. 4) despite prolonged tail bleeding times observed in a subgroup of the animals, which confirms that there is no clear correlation between bleeding time and risk (27). These findings are in line with our recent observation that inhibition of the GPIb–GPVI axis is protective in this model, whereas integrin αIIbβ3 (GPIIb/IIIa) inhibition is not but is associated with excess intracranial bleeding (3), which corresponds well with data from clinical studies in stroke patients (26). It is important to note, however, that data obtained in the mouse tMCAO model cannot be directly extrapolated to the human situation, as differences in the pathomechanisms may exist.

Overall, the phenotype of mice with *Stim1*$^{-/-}$ platelets is similar to that of mice lacking functional GPVI or mice treated with antibodies that block the von Willebrand factor binding site on GPIbα, which show severe defects in thrombus formation under flow, protection from arterial thrombus formation, and ischemic brain damage, but which only exhibit a limited risk for bleeding complications (3, 28). This supports the notion that SOCE is particularly important for GPIb–GPVI–ITAM signaling pathways in platelets, which is in line with the well-documented function of STIM1 in ITAM signaling in T cells and mast cells (10, 22).

Collectively, the results presented in this paper establish STIM1 as an essential mediator of platelet activation that is of critical importance during arterial thrombosis and ischemic brain infarction but not normal hemostasis. These findings may open the way for the development of novel highly effective and safe antithrombotics.

MATERIALS AND METHODS

Mice. Animal studies were approved by the district government of Lower Franconia (Bezirksregierung Unterfranken). The generation of *Stim1*$^{-/-}$ mice was as follows. A gene trap embryonic stem (ES) cell line containing an insertional disruption in the *Stim1* gene (RRS558; clone no. IRAK-p961K1818Q; imaGenes) was purchased from BayGenomics. Male chimeras from this ES cell line were bred to C57BL/6 females to generate *Stim1*$^{+/-}$ mice,

which were intercrossed to produce *Stim1*$^{-/-}$ mice. In the ES cells, the gene trap vector pCMV-SPORT6, which is composed of a splice-acceptor site followed by a "βGeo" cassette encoding a fusion of β-galactosidase and neomycin phosphotransferase II, was inserted 600 bp downstream of exon 7, into intron 7 of the *Stim1* gene. The integration site was confirmed by PCR and sequencing of the amplified genomic DNA fragment using exon 7 forward (5′-gctgcacaaggcccaggagg-3′) and geo1 reverse (5′-atcggcctcaggaagatcgc-3′) primers. The transcript would result in the generation of a fusion protein between truncated Stim1 (extracellular region plus transmembrane domain) and β-galactosidase. This fusion protein was, however, not detectable in platelets by Western blotting using anti–β-galactosidase antibodies or anti-STIM1 antibodies that recognize the N terminus of the protein (GOK/Stim1, clone 44; BD Bioscience) (11), suggesting that it is rapidly degraded. For the generation of bone marrow chimeras, 5–6-wk-old C57BL/6 female mice were lethally irradiated with a single dose of 10 Gy, and bone marrow cells from 6-wk-old wild-type or *Stim1*$^{-/-}$ mice were injected intravenously into the irradiated mice (4×10^6 cells per mouse). 4 wk after transplant, platelet counts were determined and STIM1 deficiency was confirmed by Western blotting. All recipient animals received acidified water containing 2 g/liter neomycin sulfate for 6 wk after transplantation.

Chemicals and antibodies. Anesthetic drugs used included medetomidine (Pfizer), midazolam (Roche), and fentanyl (Janssen-Cilag GmbH). For antagonists, atipamezol (Pfizer) and flumazenil and naloxon (both purchased from Delta Select GmbH) were used according to local authority regulations. ADP (Sigma-Aldrich), U46619 (Qbiogene), thrombin (Roche), collagen (Kollagenreagent Horm; Nycomed), and TG (Invitrogen) were purchased as indicated. Monoclonal antibodies conjugated to FITC or PE, or DyLight 488 were obtained from Emfret Analytics. The JON/A-PE antibody preferentially binds to the high affinity conformation of mouse integrin αIIbβ3 (Emfret Analytics). Anti-STIM1 monoclonal antibodies were purchased from BD Biosciences (GOK/Stim1, clone 44) and Abnova (clone 5A2).

Intracellular calcium measurements. Platelet intracellular calcium measurements were performed as previously described (29). In brief, platelets isolated from blood were washed, suspended in Tyrode's buffer without calcium, and loaded with 5 μM Fura-2/AM in the presence of 0.2 μg/ml Pluronic F-127 (Invitrogen) for 30 min at 37°C. After labeling, platelets were washed once and resuspended in Tyrode's buffer containing 0.5 mM Ca^{2+} or 1 mM EGTA. Stirred platelets were activated with agonists, and fluorescence was measured with a fluorimeter (LS 55; PerkinElmer). Excitation was alternated between 340 and 380 nm, and emission was measured at 509 nm. Each measurement was calibrated using Triton X-100 and EGTA.

Platelet aggregation and flow cytometry. Washed platelets (200 μl with 0.5×10^6 platelets/μl) were analyzed in the presence of 70 μg/ml human fibrinogen. Transmission was recorded on a four-channel aggregometer (Fibrintimer; APACT) for 10 minutes and was expressed in arbitrary units, with buffer representing 100% transmission. For flow cytometry, heparinized whole blood was diluted 1:20 and incubated with the appropriate fluorophore-conjugated monoclonal antibodies for 15 min at room temperature and analyzed on a FACSCalibur (Becton Dickinson).

Adhesion under flow conditions. Rectangular coverslips (24 × 60 mm) were coated with 0.2 mg/ml fibrillar type I collagen (Nycomed) for 1 h at 37°C and blocked with 1% BSA. Heparinized whole blood was labeled with a DyLight 488–conjugated anti-GPIX Ig derivative at 0.2 μg/ml, and perfusion was performed as previously described (16). Image analysis was performed off-line using Metavue software (Visitron). Thrombus formation was expressed as the mean percentage of total area covered by thrombi, and as the mean integrated fluorescence intensity per square millimeter.

Bleeding time. Mice were anesthetized and a 3-mm segment of the tail tip was removed with a scalpel. Tail bleeding was monitored by gently absorbing blood with filter paper at 20-s intervals without making contact with the wound site. When no blood was observed on the paper, bleeding was determined to have ceased. Experiments were stopped after 20 min.

Intravital microscopy of thrombus formation in $FeCl_3$-injured mesenteric arterioles. 4 wk after bone marrow transplantations, chimeras were anesthetized and the mesentery was exteriorized through a midline abdominal incision. 35–60-μm-diameter arterioles were visualized at 10× with an inverted microscope (Axiovert 200; Carl Zeiss, Inc.) equipped with a 100-W HBO fluorescent lamp source and a camera (CoolSNAP-EZ; Visitron). Digital images were recorded and analyzed off-line using Metavue software. Injury was induced by topical application of a 3-mm^2 filter paper saturated with 20% $FeCl_3$ for 10 s. Adhesion and aggregation of fluorescently labeled platelets (DyLight 488–conjugated anti-GPIX Ig derivative) in arterioles was monitored for 30 min or until complete occlusion occurred (blood flow stopped for >1 min).

Aorta occlusion model. A longitudinal incision was performed to open the abdominal cavity of anesthetized mice and expose the abdominal aorta. An ultrasonic flow probe was placed around the vessel, and thrombosis was induced by a single firm compression with a forceps. Blood flow was monitored until complete occlusion occurred or 30 min had elapsed.

MCA occlusion model. Experiments were conducted on 10–12-wk-old *Stim1*$^{-/-}$ or control chimeras according to previously published recommendations for research in mechanism-driven basic stroke studies (30). tMCAO was induced under inhalation anesthesia using the intraluminal filament (Doccol Company) technique (3). After 60 min, the filament was withdrawn to allow reperfusion. For measurements of ischemic brain volume, animals were killed 24 h after induction of tMCAO, and brain sections were stained with 2% TTC (Sigma-Aldrich). Brain infarct volumes were calculated and corrected for edema, as previously described (3). Neurological function and motor function were assessed by two independent and blinded investigators 24 h after tMACO, as previously described (3).

Assessment of infarction and hemorrhage by MRI. MRI was performed 24 h and 7 d after transient ischemia on a 1.5 T unit (Vision; Siemens) under inhalation anesthesia. A custom-made dual-channel surface coil was used for all measurements (A063HACG; Rapid Biomedical). The MR protocol included a coronal T2-w sequence (slice thickness = 2 mm) and a coronal T2-w gradient echo constructed interference in steady state (CISS) sequence (slice thickness = 1 mm). MR images were transferred to an external workstation (Leonardo; Siemens) for data processing. The visual analysis of infarct morphology and the search for eventual intracerebral hemorrhage were performed in a blinded manner. Infarct volumes were calculated by planimetry of hyperintense areas on high resolution CISS images.

Histology. Formalin-fixed brains embedded in paraffin (HistoLab) were cut into 4-μm-thick sections and mounted. After removal of paraffin, tissues were stained with hematoxylin and eosin (Sigma-Aldrich).

Statistics. Results from at least three experiments per group are presented as means ± SD. Differences between wild-type and *Stim1*$^{-/-}$ groups were assessed by the two-tailed Student's *t* test. For the stroke model, results are presented as means ± SD. Infarct volumes and functional data were tested for Gaussian distribution with the D'Agostino and Pearson omnibus normality test and then analyzed using the two-tailed Student's *t* test. For statistical analysis, PrismGraph 4.0 software (GraphPad Software, Inc.) was used. $P < 0.05$ was considered statistically significant.

Online supplemental material. Videos 1 and 2 show representative time-lapse videos of in vivo thrombus formation in control and *Stim1*$^{-/-}$ chimeras. Online supplemental material is available at http://www.jem.org/cgi/content/full/jem.20080302/DC1.

We thank Michael Bösl for help with the generation of the mice, Ronmy Rivera Galdos and Madeleine Austinat for histology, and David Gailani for critically reading the manuscript.

This work was supported by the Rudolf Virchow Center and the Deutsche Forschungsgemeinschaft (Sonderforschungsbereich 688, A1 and B1, and grant Ni556/7-1 to B. Nieswandt).

The authors declare that they have no competing financial interests.

Submitted: 14 February 2008
Accepted: 27 May 2008

REFERENCES

1. Ruggeri, Z.M. 2002. Platelets in atherothrombosis. *Nat. Med.* 8: 1227–1234.
2. Bhatt, D.L., and E.J. Topol. 2003. Scientific and therapeutic advances in antiplatelet therapy. *Nat. Rev. Drug Discov.* 2:15–28.
3. Kleinschnitz, C., M. Pozgajova, M. Pham, M. Bendszus, B. Nieswandt, and G. Stoll. 2007. Targeting platelets in acute experimental stroke: impact of glycoprotein Ib, VI, and IIb/IIIa blockade on infarct size, functional outcome, and intracranial bleeding. *Circulation.* 115:2323–2330.
4. Sachs, U.J., and B. Nieswandt. 2007. In vivo thrombus formation in murine models. *Circ. Res.* 100:979–991.
5. Berridge, M.J., M.D. Bootman, and H.L. Roderick. 2003. Calcium signalling: dynamics, homeostasis and remodelling. *Nat. Rev. Mol. Cell Biol.* 4:517–529.
6. Feske, S. 2007. Calcium signalling in lymphocyte activation and disease. *Nat. Rev. Immunol.* 7:690–702.
7. Bird, G.S., O. Aziz, J.P. Lievremont, B.J. Wedel, M. Trebak, G. Vazquez, and J.W. Putney Jr. 2004. Mechanisms of phospholipase C-regulated calcium entry. *Curr. Mol. Med.* 4:291–301.
8. Liou, J., M.L. Kim, W.D. Heo, J.T. Jones, J.W. Myers, J.E. Ferrell Jr., and T. Meyer. 2005. STIM is a Ca2+ sensor essential for Ca2+-store-depletion-triggered Ca2+ influx. *Curr. Biol.* 15:1235–1241.
9. Zhang, S.L., Y. Yu, J. Roos, J.A. Kozak, T.J. Deerinck, M.H. Ellisman, K.A. Stauderman, and M.D. Cahalan. 2005. STIM1 is a Ca2+ sensor that activates CRAC channels and migrates from the Ca2+ store to the plasma membrane. *Nature.* 437:902–905.
10. Oh-Hora, M., M. Yamashita, P.G. Hogan, S. Sharma, E. Lamperti, W. Chung, M. Prakriya, S. Feske, and A. Rao. 2008. Dual functions for the endoplasmic reticulum calcium sensors STIM1 and STIM2 in T cell activation and tolerance. *Nat. Immunol.* 9:432–443.
11. Baba, Y., K. Nishida, Y. Fujii, T. Hirano, M. Hikida, and T. Kurosaki. 2008. Essential function for the calcium sensor STIM1 in mast cell activation and anaphylactic responses. *Nat. Immunol.* 9:81–88.
12. Feske, S., Y. Gwack, M. Prakriya, S. Srikanth, S.H. Puppel, B. Tanasa, P.G. Hogan, R.S. Lewis, M. Daly, and A. Rao. 2006. A mutation in Orai1 causes immune deficiency by abrogating CRAC channel function. *Nature.* 441:179–185.
13. Huang, G.N., W. Zeng, J.Y. Kim, J.P. Yuan, L. Han, S. Muallem, and P.F. Worley. 2006. STIM1 carboxyl-terminus activates native SOC, I(crac) and TRPC1 channels. *Nat. Cell Biol.* 8:1003–1010.
14. Grosse, J., A. Braun, D. Varga-Szabo, N. Beyersdorf, B. Schneider, L. Zeitlmann, P. Hanke, P. Schropp, S. Muhlstedt, C. Zorn, et al. 2007. An EF hand mutation in Stim1 causes premature platelet activation and bleeding in mice. *J. Clin. Invest.* 117:3540–3550.
15. Lopez, J.J., G.M. Salido, J.A. Pariente, and J.A. Rosado. 2006. Interaction of STIM1 with endogenously expressed human canonical TRP1 upon depletion of intracellular Ca2+ stores. *J. Biol. Chem.* 281:28254–28264.
16. Nieswandt, B., C. Brakebusch, W. Bergmeier, V. Schulte, D. Bouvard, R. Mokhtari-Nejad, T. Lindhout, J.W. Heemskerk, H. Zirngibl, and R. Fassler. 2001. Glycoprotein VI but not alpha2beta1 integrin is essential for platelet interaction with collagen. *EMBO J.* 20:2120–2130.
17. Murray, C.J., and A.D. Lopez. 1997. Mortality by cause for eight regions of the world: Global Burden of Disease Study. *Lancet.* 349:1269–1276.
18. Zhang, Z.G., L. Zhang, W. Tsang, A. Goussev, C. Powers, K.L. Ho, D. Morris, S.S. Smyth, B.S. Coller, and M. Chopp. 2001. Dynamic platelet accumulation at the site of the occluded middle cerebral artery and in downstream microvessels is associated with loss of microvascular integrity after embolic middle cerebral artery occlusion. *Brain Res.* 912:181–194.
19. Choudhri, T.F., B.L. Hoh, H.G. Zerwes, C.J. Prestigiacomo, S.C. Kim, E.S.J. Connolly, G. Kottirsch, and D.J. Pinsky. 1998. Reduced microvascular thrombosis and improved outcome in acute murine stroke by inhibiting GP IIb/IIIa receptor-mediated platelet aggregation. *J. Clin. Invest.* 102:1301–1310.
20. Hassock, S.R., M.X. Zhu, C. Trost, V. Flockerzi, and K.S. Authi. 2002. Expression and role of TRPC proteins in human platelets: evidence that TRPC6 forms the store-independent calcium entry channel. *Blood.* 100:2801–2811.
21. Parvez, S., A. Beck, C. Peinelt, J. Soboloff, A. Lis, M. Monteilh-Zoller, D.L. Gill, A. Fleig, and R. Penner. 2008. STIM2 protein mediates distinct store-dependent and store-independent modes of CRAC channel activation. *FASEB J.* 22(3):752–761.
22. Vig, M., W.I. Dehaven, G.S. Bird, J.M. Billingsley, H. Wang, P.E. Rao, A.B. Hutchings, M.H. Jouvin, J.W. Putney, and J.P. Kinet. 2008. Defective mast cell effector functions in mice lacking the CRACM1 pore subunit of store-operated calcium release-activated calcium channels. *Nat. Immunol.* 9:89–96.
23. Watson, S.P., N. Asazuma, B. Atkinson, O. Berlanga, D. Best, R. Bobe, G. Jarvis, S. Marshall, D. Snell, M. Stafford, et al. 2001. The role of ITAM- and ITIM-coupled receptors in platelet activation by collagen. *Thromb. Haemost.* 86:276–288.
24. Offermanns, S. 2006. Activation of platelet function through G protein-coupled receptors. *Circ. Res.* 99:1293–1304.
25. Jackson, S.P., W.S. Nesbitt, and S. Kulkarni. 2003. Signaling events underlying thrombus formation. *J. Thromb. Haemost.* 1:1602–1612.
26. Adams, H.P., Jr., M.B. Effron, J. Torner, A. Davalos, J. Frayne, P. Teal, J. Leclerc, B. Oemar, L. Padgett, E.S. Barnathan, and W. Hacke. 2008. Emergency administration of abciximab for treatment of patients with acute ischemic stroke: results of an international phase III trial. Abciximab in Emergency Treatment of Stroke Trial (AbESTT-II). *Stroke.* 39:87–99.
27. Rodgers, R.P., and J. Levin. 1990. A critical reappraisal of the bleeding time. *Semin. Thromb. Hemost.* 16:1–20.
28. Massberg, S., M. Gawaz, S. Gruner, V. Schulte, I. Konrad, D. Zohlnhofer, U. Heinzmann, and B. Nieswandt. 2003. A crucial role of glycoprotein VI for platelet recruitment to the injured arterial wall in vivo. *J. Exp. Med.* 197:41–49.
29. Heemskerk, J.W., M.A. Feijge, E. Rietman, and G. Hornstra. 1991. Rat platelets are deficient in internal Ca2+ release and require influx of extracellular Ca2+ for activation. *FEBS Lett.* 284:223–226.
30. Dirnagl, U. 2006. Bench to bedside: the quest for quality in experimental stroke research. *J. Cereb. Blood Flow Metab.* 26:1465–1478.